International Journal of Science and Research (IJSR)
ISSN: 2319-7064
SJIF (2022): 7.942

Effect of Additives on the Thermal Decomposition Process of Zinc Citrate Complexes to ZnO

Harsha P. Uskaikar

PES'S RSN College of Arts & Science, Farmagudi, Ponda, Goa. 403001, India
E-mail: *harshapundalik[at]gmail.com*
Tel: 08326529933
Fax: 08322335296

Abstract: ***Nanocrystalline ZnO has been synthesized through a citrate gel decomposition technique. The technique was modified by addition of additives such as ethylene glycol and CDTA (1,2 Cyclohexylenedinitrotetracetic acid). The conditions for obtaining nanocrystalline ZnO have been optimized. The influence of interaction additives-precursor gels on the evolution of structural features and particle morphology of ZnO have been studied by Infra red spectroscopy, thermal analysis TG-DTA & SEM. These properties of ZnO powders have been further supported by XRD. X-ray diffraction patterns showed the formation of wurtzite structure. The SEM analysis revealed that the morphologies of the as prepared ZnO were nanocrystalline, spherical in shape. When ethylene glycol is used as an additive particle size was found to be equal to 54 nm and in case of CDTA the particle size was 50 nm. It is found that additives addition was not much influencing the formation of ZnO nanostructure.***

Keywords: XRD, SEM, FTIR, ZnO, Combustion technique, Particle size

1. Introduction

Zinc oxide (ZnO) is a II-VI semiconductor material with band gap energy of 3.35 eV and a higher free exciton binding energy of 60 meV. Presently, development of ZnO nano structures such as nano scale spherical particles, tubes, rods, arrays, sheets and hollow spherical particles have been given more importance due to their useful properties, such as optical absorption and emission [1], conductivity [2], photocatalyst [3] and sensitivity to gases [4]. Various ZnO nanostructures have been synthesized and utilized as gas sensors, such as nanoparticles [5], nanorods [6,7], nanowires [8,9], nanobelts [10], nanoplates [11] hollow spheres[12], nanoflakes[13]and shuttle like nano micro rods[14].Chemical methods such as hydrothermal, solvothermal and sol gel synthesis techniques have been reported extensively for preparation of nano ZnO [15,16]. Combustion synthesis is capable technique for obtaining ZnO powders with controlled size and shape [17]. However, in this technique, the various processing parameters such as the oxidizer to fuel ratio, chemical nature of the starting precursor [e.g nitrates, sulphates and acetates], fuel source, pH of the precursor solution and the mode of heating have to be carefully optimized for producing fully crystalline ZnO nano particles. For example, when glycine was used as the fuel, hexagonal nanocrystalline ZnO was obtained [18]. Combustion synthesis and microwave method [19] were used to prepare citrate gel conventionally. When the combustion synthesis was applied to zinc metal, zinc nitrate and glycine mixtures, resultant ZnO morphology varied from rods, needles to tetra-pods [20]. ZnO nanopowder was prepared by using different fuels like glycine, Urea & citric acid [21] Citrate nitrate process was also used in the preparation of nanoparticles of oxide [22]. Lot of work has been reported on use of citric acid as ligand in ZnO preparation in other words pechini method for preparation of zinc oxide is much exploited [23]. In the present study, combustion synthesis has been considered by using citric acid and zinc nitrate as fuel and oxidizer and ethylene glycol and CDTA (1,2 Cyclohexylenedinitrotetracetic acid) as additives. The effect of additives on the ZnO nanostructure and particle morphology have been studied.

2. Experimental

Materials

All reagents used were AR grade, $Zn(NO_3)_2.4H_2O$, citric acid & ethylene glycol from S. d fine & CDTA from Merck were used as such without further purification.

Synthesis

Method 1 In a typical experiment, $Zn(NO_3)_2.4H_2O$ and citric acid reactants in the mole ratios 1:2 and dissolved in a known quantity of ethylene glycol. The reactant solutions were mechanically stirred for almost 18 hrs at 110^oC (until gel formation). From the TG analysis, it was established that a temperature of at least 500^oC was required to obtain fully-crystalline ZnO. Dried gel precursor was then sintered at 470^oC for 3h.Sample was coded as **A.** Fig. 1 flowsheet shows the synthesis of A.

Method 2 In a typical experiment, $Zn(NO_3)_2.4H_2O$ and citric acid reactants in the mole ratios 1:2 and dissolved in a known quantity of CDTA. The reactant solutions were mechanically stirred for almost 18 hrs at 110^oC (until gel formation). From the TG analysis, it was established that a temperature of at least 500^oC was required to obtain fully-crystalline ZnO. Dried gel precursor was then sintered at 510^oC for 3h.Sample was coded as **B**.

Fig. 2 flowsheet shows the synthesis of B.

Instrumentation

The infrared (IR) spectra were recorded on a Shimadzu DR 8031 using KBr pellet technique in the range of 400–4000 cm^{-1}.To understand the complete thermal decomposition of the gels, the dried precursor gel was subjected to thermo

gravimetry [TG] using a TG/DT-50H (SHIMADZU, Japan) at a constant heat flow of 10Kminutes^{-1} in an air atmosphere up to 600^{o}C The crystalline nature and phase evolution of the as prepared and calcined ZnO powders were studied by powder X-ray diffraction using a Philips, X'pert Pro with a monochromator on the diffraction beam side (Cu Kα radiation, $\lambda = 0.154$ nm). The crystallite size of the powder was calculated using Scherer's equation [24]. The morphology of ZnO powder was probed using scanning electron microscopy (SEM). The SEM studies were carried out by a JEOL 5600 SL-SEM, operated at 15 KV.

3. Result & Discussion

The citrate gel decomposition process is better known as a thermally induced anionic oxidation-reduction reaction [25]. When citric acid is mixed with precursor salt in an aqueous solution in specific ratios or concentrations, chelates are formed between metal ions facilitating atomic scale distribution of ions in a polymer network. Heating of this resin causes the breakdown of the polymer and a solid amorphous precursor material is finally obtained. On subsequent heating between 500 to 900^{o}C, cations are oxidized to form the respective metal oxides [25].

Fig 3 & 4 shows the IR spectrum of A & B. IR spectrum of A shows few peaks prominently showing characteristic bands of Zn-O vibrations which appear at 444 and 457 cm^{-1} and broad peak around 3500 cm^{-1} which can be assigned to the presence of the O-H stretching mode of hydroxyl group [26]. For B more absorption peaks other than between 400-500cm^{-1} are observed. The bands at 1249 and 1037 cm^{-1} could be attributed to nitrate ions. A weak band at 1242 and 1612 cm^{-1}, indicative of the presence of residual organic compounds. These bands were no longer observed as the materials were calcined at 700℃ reported by [27, 28] suggesting the decomposition of the residual material of the synthesis process.

The TG curves obtained for sample A and B are shown in Fig. 5 & 6. Three major decomposition steps were observed. In the first step a drastic mass loss occurred up to 240^{o}C. At this temperature melting of the citric acid fuel followed by the decomposition are usually expected. Precisely, the citric acid melting is seen at 157^{o}C but it decomposes strongly between the temperatures 215 to 220^{o}C. The mass loss is also associated partly with the dehydration of the free water molecules present in the gel network. The total mass loss of 10 % is seen in the first stage. The second step mass loss of 61% took place between 240 to 370^{o}C and in this temperature range, the decomposition of metal complexes to metal hydroxides, decomposition of free nitrates, formation of by products such as ammonium citrate were expected to occur. Nitrates thermally decompose below 350^{o}C with the evolution of nitrogen oxides [NO_2, NO and N_2O_5] [29]. The TG pattern confirms that there is no major mass loss above 540^{o}C. Although the citric acid undergoes almost complete gasification below 400^{o}C, the thermal analysis data in air shows the combustion of a small amount of carbonaceous material at 471^{o}C. The third stage above 400^{o}C is associated with the loss of free carbon as CO_2 and dehydroxylation of zinc hydroxide into ZnO. As evidenced from the curve, an intermediate decomposition between 250 to 300^{o}C is crucial, because at this range the nitrate and citrate gel networks collapse and primary zinc hydroxide nuclei formation starts in the precursor gel mass. The nuclei size formed should be controlled because it gets converted to crystalline ZnO upon further calcination. TG analysis, confirmed that the precursor gel became fully-crystalline ZnO powders only above 400^{o}C. According to Farbun et al [30] $Zn(C_6H_7O_7)_2$ which is formed in compound is unstable and above 250^{o}C decomposes to itaconic acid and zinc citraconate $ZnC_5H_4O_4$, ethylene glycol containing precursors require higher thermal treatment temperatures. Which can also be proved on the basis of TG curves TG curve of A shows 90% decomposition whereas curve B shows mass loss 100%. Surprisingly Curve B shows 100% decomposition where a multidentate ligand like CDTA is used.

From TG-DTA it is understood that ZnO is formed at 470^{o}C when ethylene glycol is used as an additive and at 510^{o}C when CDTA is used. Mass loss %, DTA Temperature, crystallite diameter & Particle size obtained from SEM is shown in Table 1. It looks additives are not helping much in reducing the formation temperature of ZnO but from SEM data it looks that surface morphology and particle size gets altered. The powder crystallanity is confirmed from the X-ray diffraction analysis as presented in Fig. 7 & 8 Both samples possess the ZnO wurtzite structure [31, 32, 33]. Without any other impurity peaks, characteristic ZnO peaks are clearly observed at 36.2°, 31.7°, 34.3°, 47.5°, 56.5°, 62.8°, 66.3°, 67.8° and 69.0°, corresponding to the (101), (100), (002), (102), (110), (200), (112), (201) and (004) planes, respectively. The crystallite size is calculated from the Scherer's formula as 37 nm for A & 50 nm for B. When CDTA is added as an additive the crystallites tend to agglomerate as a porous chain structure shown by the SEM images, where as when ethylene glycol was used as an additive fine spherical nanocrystals were formed with particle size 54 nm for A and 50 nm for B. SEM micrographs for A & B are shown in Fig. 9 & 10. In B uniform spherical morphology was not observed, but a porous structure was observed. Thus showing addition of CDTA as an additive helps in developing porous ZnO structure and altering the surface morphology.

4. Conclusion

ZnO was synthesized successfully by using Zinc nitrate, citric acid with ethylene glycol and CDTA as additives. IR spectra confirms the presence of Zn-O bond in between 400-500 Cm^{-1}. TG-DTA curve shows that ZnO was formed at 470^{o}C when ethylene glycol was used as an additive and at 510^{o}C when CDTA was used. It looks additives are not helping much in reducing the formation temperature of nanocrystalline zinc oxide. From XRD patterns formation of wurtzite phase was confirmed, crystallite diameter from XRD was found to be 37 & 50nm and from SEM particle size was found to be 54 & 50 nm.

Acknowledgments
Author is greatful to Dr. Narendra Ghosh, Dr. Bhanudas Naik of BITS Pilani – Goa Campus, for Thermal and XRD analysis. Dr. Rahul Mohan & Sahina Gazi National Centre for Antartica and Ocean Research (NCAOR), Vasco-da - gama for SEM analysis.

References

[1] Xu P, Wen X, Zheng Z, Cox G, Zhu H. Two-photon optical characteristics of zinc oxide in bulk low dimensional and nanoforms. J Lumin 2007;126:641-3.

[2] Lu JJ, Lu YM, Tasi SI, Hsiung TL, Wang HP, Jang LY. Conductivity enhancement and semiconductor–metal transition in Ti-doped ZnO films. Opt Mater. 2007;291:1548-52.

[3] Zhang YY, Mu J. One-pot synthesis, photoluminescence, and photocatalysis of Ag/ZnO Composites. J Colloid Interface Sci. 2007; 309: 478-84.

[4] Ghimbeu CM, Schoonman J, Lumbreras M, Siadat M. Electrostatic spradeposited zinc oxide films for gas sensor applications. Appl Surf Sci. 2007; 253;7483-9.

[5] Xu J, Pan Q, Shun Y, Tian Z. Grain size control and gas sensing properties of ZnO gas sensor. Sens. Actuators B. 2000; 66:277–9.

[6] Han N, Hu P, Zuo A, Zhang D, Tian Y, Chen Y. Photoluminescence investigation on the gas sensing property of ZnO nanorods prepared by plasmaenhanced CVD method. Sens Actuators B. 2010;145:114–9.

[7] Zhang H, Wu J, Zhai C, Du N, Ma X, Yang D. From ZnO nanorods to 3D hollow microhemispheres: solvothermal synthesis, photoluminescence and gas sensor properties. Nanotechnology 2007;18:455-604.

[8] Wan Q, Li QH, Chen YJ, Wang TH, He XL, Li JP, Lin CL. Fabrication and ethanol sensing characteristics of ZnO nanowire gas sensors. Appl. Phys. Lett. 2004;84: 3654–6.

[9] Awad MA, Ibrahim MME, Ahmed MA. Synthesis and thermal stability of ZnO nanowires J Therm Anal and Calorim. 2014; 117: 635-42.

[10] Choopun S, Hongsith N, Mangkorntong P, Mangkorntong N. Zinc oxide nanobelts by RF sputtering for ethanol sensor. Physica E. 2007;39:53–56.

[11] Jing Z, Zhan J. Fabrication and gas-sensing properties of porous ZnO nanoplates. Adv. Mater. 2008;20:4547–51.

[12] Li G, Gao SX, Wang L, Ma Z, Liu S. In situ growth mechanism and the thermodynamic functions of zinc oxide nano-arrays and hierarchical structure. J Therm Anal Calorimetry. 2014;15:201-8.

[13] Li Y, Wang S, Gao H, Tan Z. Preparation and characterization of nano-ZnO flakes prepared by reactive ion exchange method. J Therm Anal Calorim. 2009;95:671-4.

[14] Zhang L, Zhao J, Zheng J, Li L, Z. Zhu. Shuttle-like ZnO nano/microrods: Facile synthesis, optical characterization and high formaldehyde sensing properties. Appl. Surf. Sci. 2011;258:711–8.

[15] Lao JY, Huang JY, Wang DZ, Ren ZF. ZnO Nanobridges and Nanonails. Nano Lett. 2003;3:235-8.

[16] Bashi AM, Alghanimi AAK, Salah H. Characterisations of synthesis of nano hybrid octyl gallate with ZnO LHS and determined its antimicrobial activities. Chemistry and Materials Research 2014;6:2224- 3224.

[17] S. Ekambaram. Combustion synthesis and characterization of new class of ZnO-based ceramic pigments. J Alloys Compd. 2005;390: L4-L6.

[18] Hwang C-C, Wu T-Y. Synthesis and characterization of nanocrystalline ZnO powders by a novel combustion synthesis method. Mater Sci Eng B. 2004; 111:197-206.

[19] Ananthakumara S, Anasa S, Ambilya J, Mangalaraja RV. Microwave assisted citrate gel combustion synthesis of ZnO Part-I: assessment of structural features. J Ceramic Processing Research 2010;1:29-34.

[20] Lin C-S, Hwang C-C, Lee W-H, Tong W-Y. Preparation of zinc oxide (ZnO) powders with different types of morphology by a combustion synthesis method. Mater Sci Eng. B. 2007;140: 31-7.

[21] Riahi-Noori N, Sarraf-Mamoory R, Alizadehb P. Mehdikhanic A. Synthesis of ZnO nano powder by a gel combustion method. J Ceramic Processing Research 9:2008 246~249.

[22] Banerjee S, Kumar A, Sujatha Devi P. Preparation of nanoparticles of oxides by the citrate–nitrate process, J Therm Anal Calorimetry 2011;104:859-867.

[23] Lin J, Yu M, Lin C, Liu X. Multiform oxide optical materials via the versatile Pechini-type sol-gel process: synthesis and characteristics. J Phys Chem C 2007; 111:5835–5845.

[24] Klug HP, Alexander LE. X-Ray Diffraction Procedures: For Polycrystalline and Amorphous Materials, 2nd Edition Wiley, New York , 1962:992.

[25] Anas S., Mangalaraja R.V., Mukundan P., Shukla S.K. and Ananthakumar S. Direct synthesis of varistor-grade doped nanocrystalline ZnO and its densification through a stepsintering technique Acta Mater. 2007; 55:5792-5801.

[26] Pholnak C, Sirisathitkul C, Suwanboon S, David James Harding. Effects of Precursor Concentration and Reaction Time on Sonochemically Synthesized ZnO Nanoparticles. Materials Research. 2014;17(2): 405-411.

[27] Silva G, Santos JC, Martinelli D, Pedrosa1 A, de Souza M, Araujo Melo D. Synthesis and Characterization of $LaNi_xCo_{1-x}O_3$ Perovskites via Complex Precursor Methods. Materials Sciences and Applications, 2010; 1: 39-45.

[28] Jung SH, Oh E, Lee KH, Yang Y, Park CG, Park WJ. Sonochemical preparation of shape-selective ZnO nanostructures. Crystal Growth and Design. 2008; 8:265-269.

[29] Kozak AJ, Wieczorek-Ciurowa K, and Kozak A. The thermal transformations in $Zn(NO_3)_2$-H_2O (1:6) system. J Therm Anal Calorimetry 2003; 74: 497-502.

[30] Farbun I, Romanova V, Kirillov Optimal S. Design of powdered nanosized oxides of high surface area and porosity using a citric acid aided route, with special reference to ZnO. J Sol-Gel Sci Technol 2013;013:3024-7.

[31] Wypych F, Arizaga GGC, Da Costa Gardolinski JEF. Intercalation and functionalization of zinc hydroxide

nitrate with mono- and dicarboxylic acids. J Colloid and Interface Sci. 2005; 283:130-138.

[32] Haase M, Weller H, Henglein A. Photochemistry and radiation chemistry of colloidal semiconductors. J Physical Chemistry B. 1988; 92:482-487.

[33] Wu L, Wu YS. Synthesis and optical characteristic of ZnO nanorod. J Materials Sci. 2007; 42:406-408.

Table 1: Showing TG/DTA data with crystallite diameter and Particle size

Samples				
	TG%	DTA Temp °C	Crystallite diameter nm	Particle size nm
A				
Step I	10	470	37	54
Step II	61			
Step III	25			
B				
Step I	14	510	50	50
Step II	77			
Step III	22			

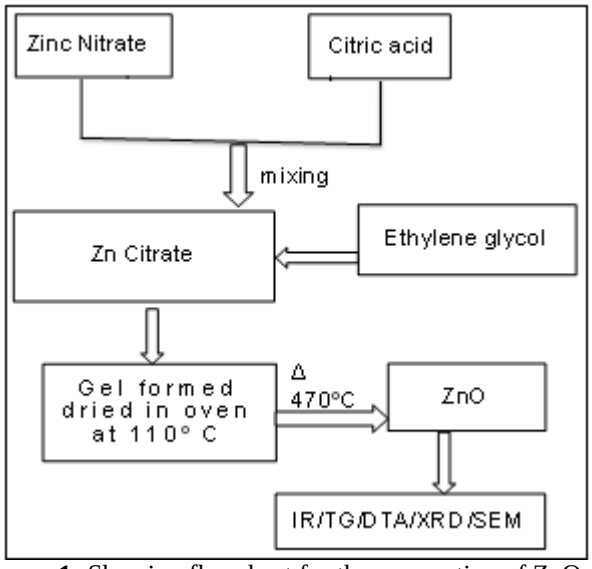

Figure 1: Showing flowsheet for the preparation of ZnO A

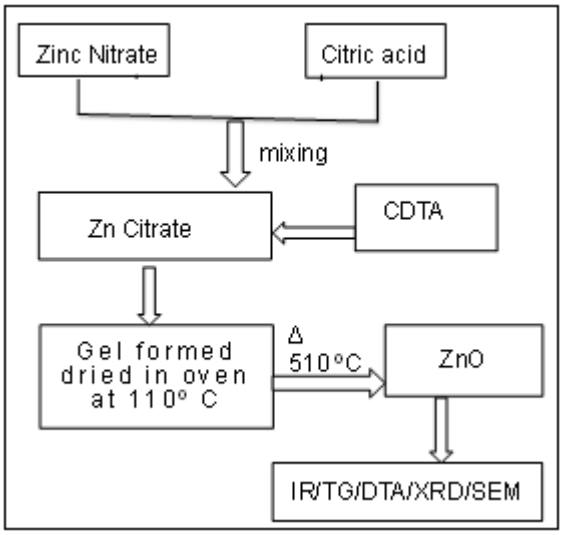

Figure 2: Showing flowsheet for the preparation of ZnO B

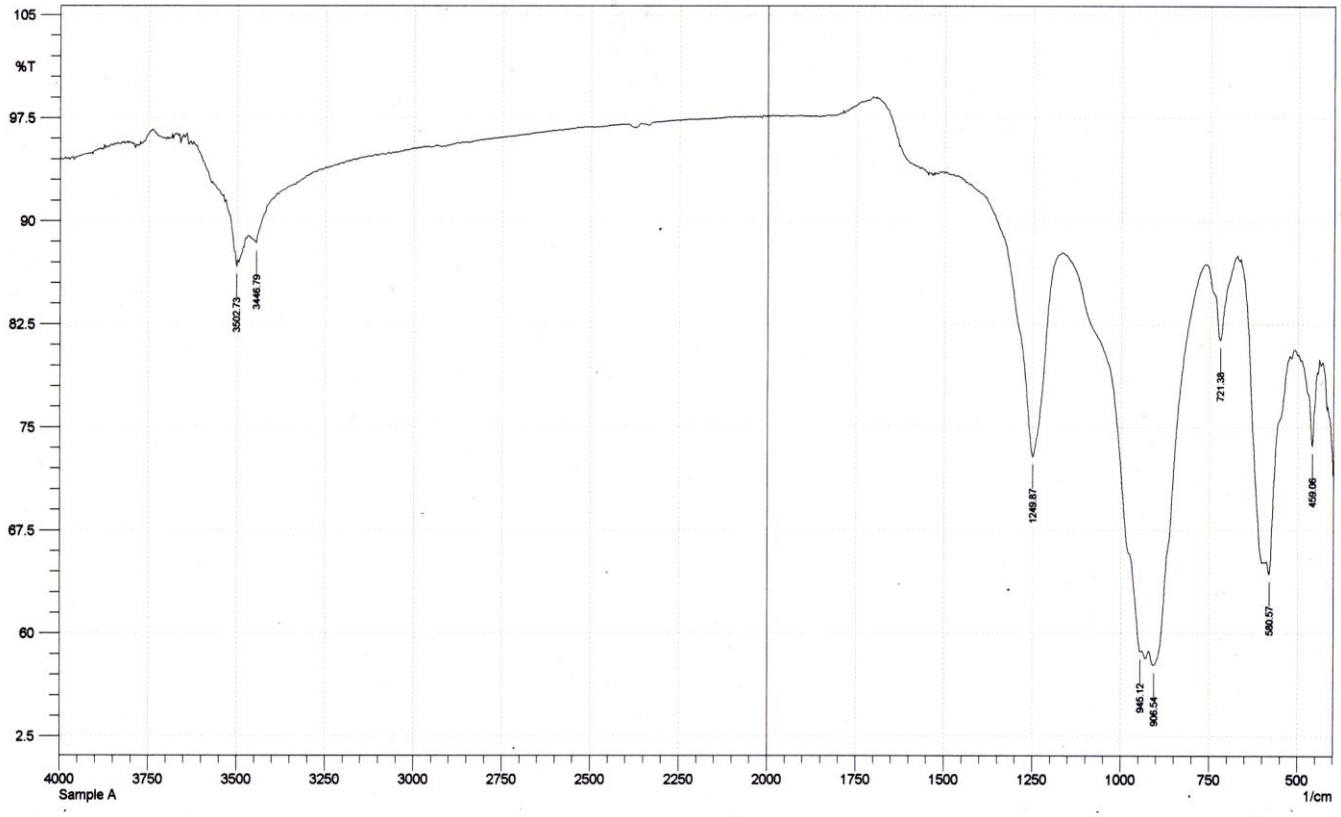

Figure 3: Infra red spectra of A

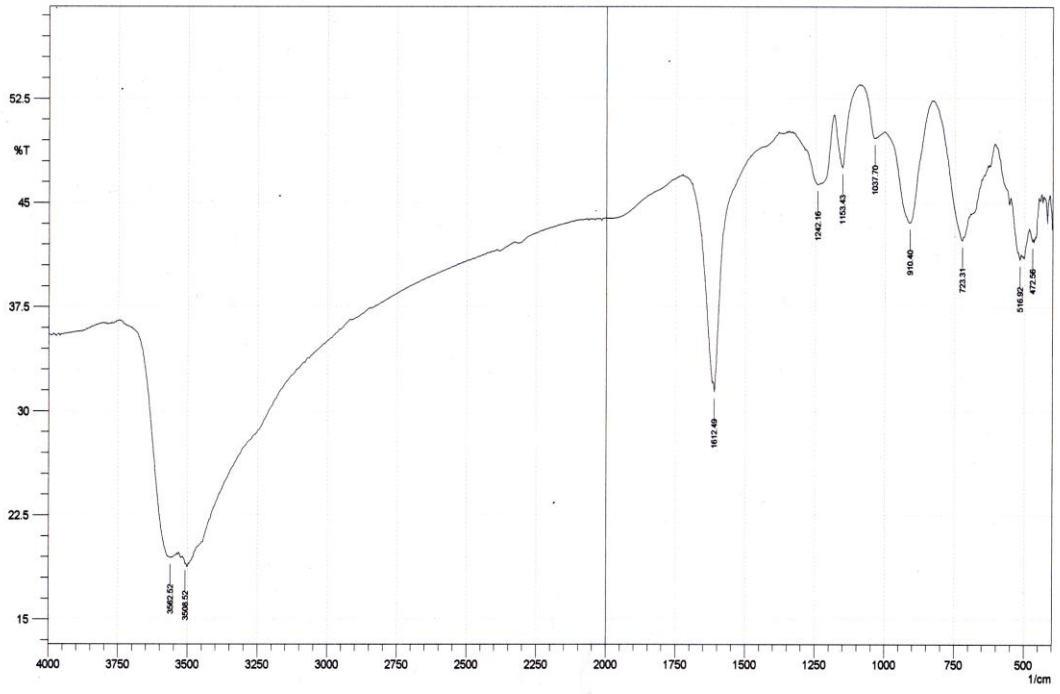

Figure 4: Infra red spectra of B

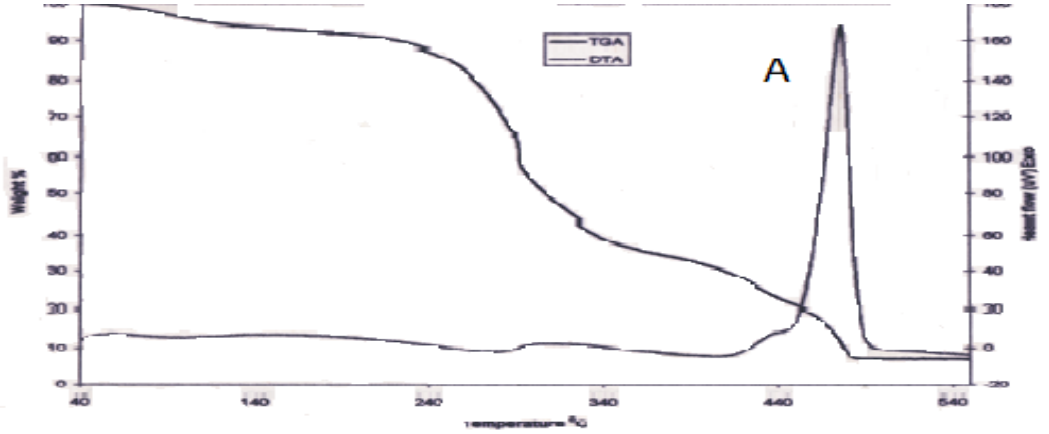

Figure 5: TG/DTA of ZnO A

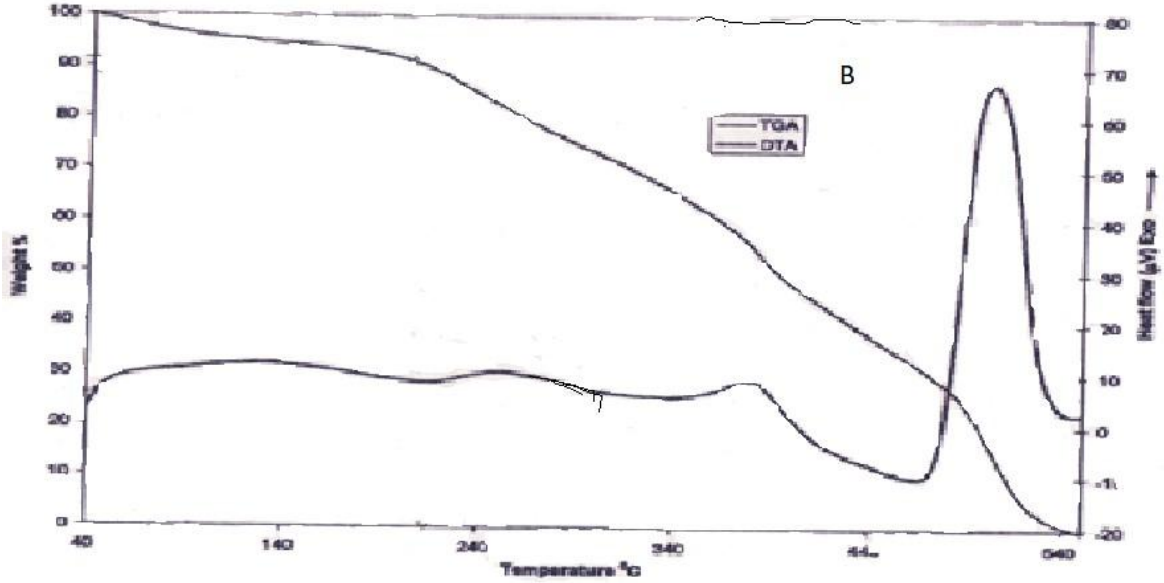

Figure 6: TG/DTA of ZnO B

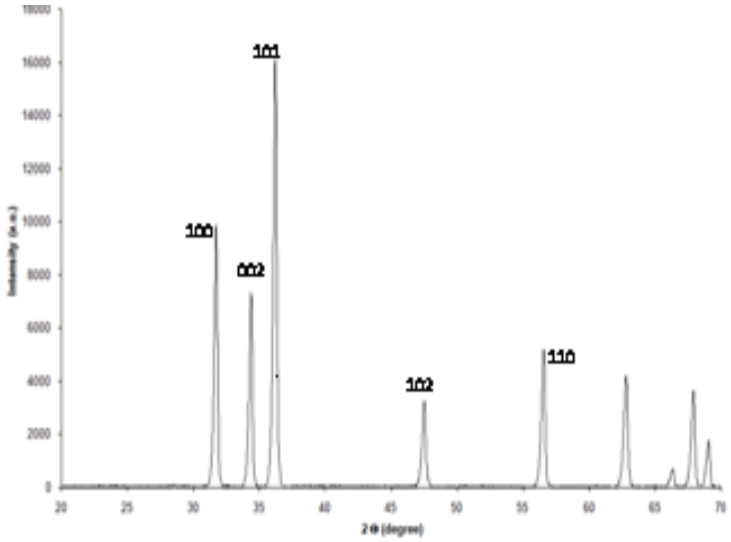

Figure 7: XRD of ZnO A

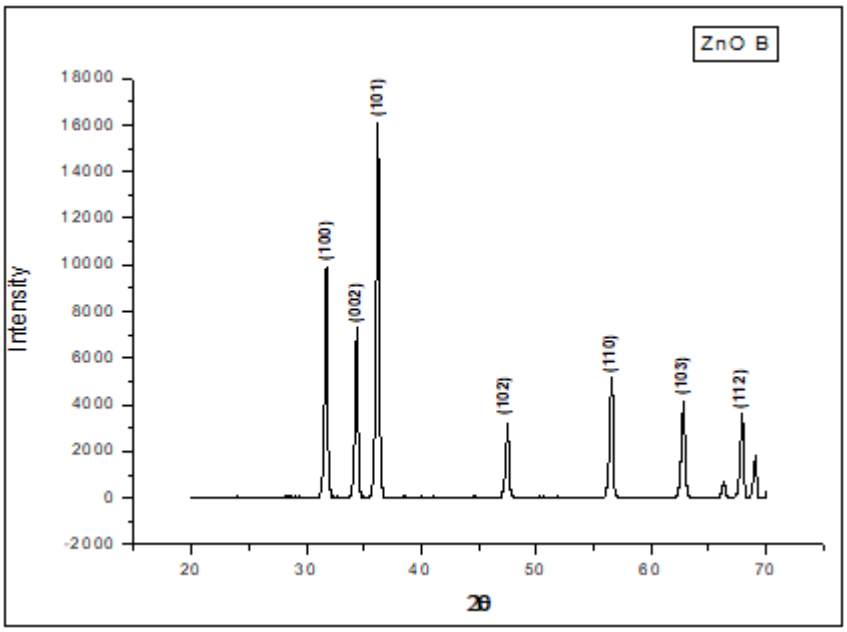

Figure 8: XRD of ZnO B

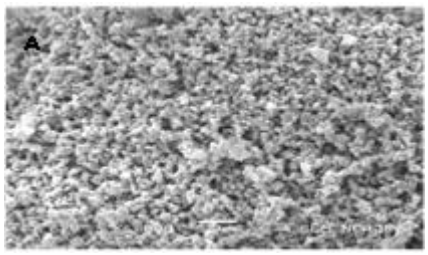

Figure 9: Scanning electron micrograph of ZnO A

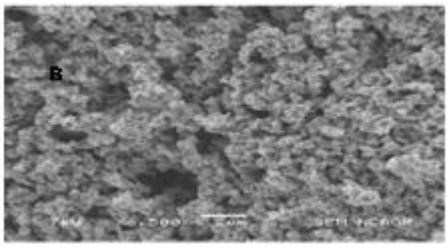

Figure 10: Scanning electron micrograph of ZnO B